Towards a Waveguide-based Single Photon Detector for Integrated Quantum Photonics Platforms

Salih Yanikgonul[1,2], Jun Rong Ong[3], Victor Leong[1], Leonid Krivitsky[1]

[1]Data Storage Institute, Agency for Science, Technology and Research, 138634, Singapore
[2]Centre for Disruptive Photonic Technologies, Nanyang Technological University, 637371, Singapore
[3]Institute of High Performance Computing, Agency for Science, Technology and Research, 138632, Singapore

Introduction

The scalability of quantum networks is a key challenge in developing practical quantum technologies. Recent developments in quantum photonics platforms show remarkable promise, but nonetheless require the coupling of light from the device to external photodetectors [1]. For a truly integrated photonics platform, these quantum devices need to be combined with on-chip single photon detectors. Here, we present our efforts towards a waveguide-coupled silicon (Si) single photon avalanche diode (SPAD), optimized for visible wavelengths. Two doping profiles are investigated.

Waveguide-coupled SPAD

Our SPAD is a 16 μm long Si rib waveguide, with an absorption of >98% at 638 nm. Input light is coupled from a silicon nitride (SiN) waveguide, which has low losses at visible wavelengths [2]. While state-of-the-art integrated photodetectors for infrared wavelengths typically use phase-matched interlayer transitions to perform this coupling [3], this is difficult to achieve in a SiN (n=2.0) to Si (n=3.8) transition due to the large difference in refractive indices. Thus, input light is end-fire coupled from the SiN waveguide to the Si SPAD in the same layer.

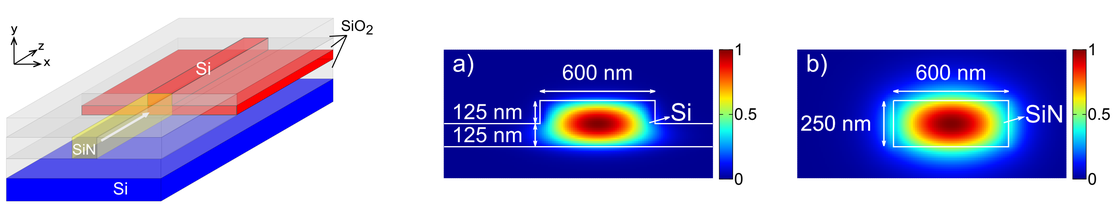

FIGURE 1: (a) Silicon SPAD coupled to a silicon nitride waveguide (b) Optical mode at 640 nm in silicon waveguide and (c) silicon nitride waveguide.

End-fire coupling efficiency is obtained from the overlap between the incoming and outgoing optical modes, and accounting for the Fresnel reflection of 10%.

$$\text{mode overlap} = \frac{|\iint E_{Si}(x,y)\, E^*_{SiN}(x,y)\, dxdy|^2}{\iint |E_{Si}(x,y)|^2 dxdy \cdot \iint |E_{SiN}(x,y)|^2 dxdy}$$

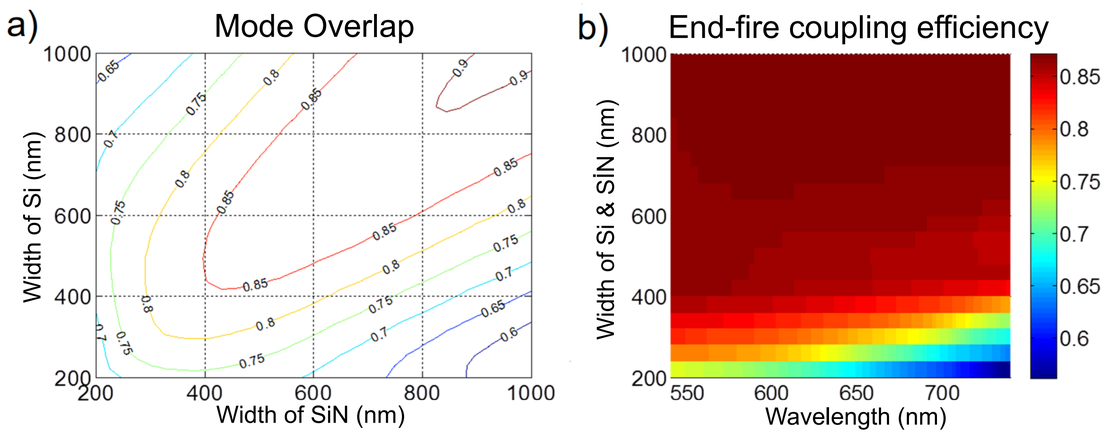

FIGURE 2: For a fixed waveguide height of 250 nm, (a) the mode overlap at 640 nm and (b) full-wave 3D FDTD simulation of the end-fire coupling efficiency.

Straight Doping Profile

The first design (Fig. 3) incorporates a single continuous depletion region along the direction of light propagation. We design the p-n+ junction such that the depletion region extends largely into the p-doped side; the absorption of a photon in the depletion region would then trigger an avalanche multiplication of electrons, which have higher ionization coefficient than holes in silicon. This placement of the p-n+ junction results in a large overlap of the depletion region and the optical waveguide mode, which yields a high detection efficiency.

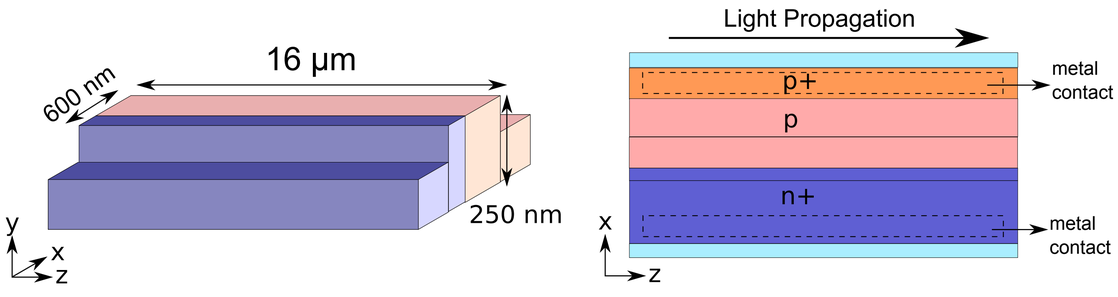

FIGURE 3: Straight doping profile.

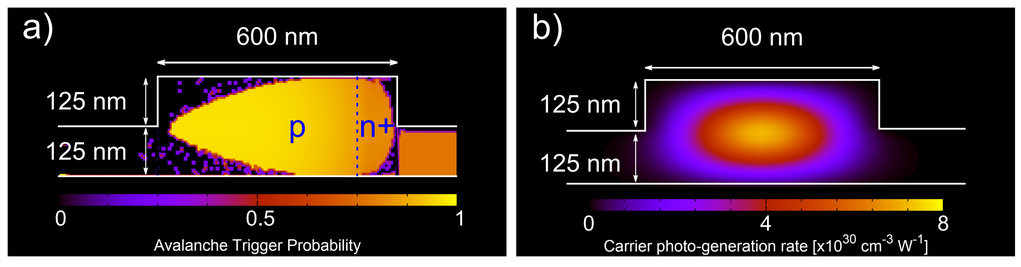

FIGURE 4: (a) Avalanche triggering probability and (b) carrier photo-generation rate for the straight doping profile.

Interdigitated Doping Profile

However, the straight doping profile requires more stringent control during fabrication, as a small misalignment of the junction will result in a large mismatch between the optical mode and the depletion region. Therefore, we study an interdigitated doping profile (Fig. 5), which is less sensitive to such fabrication errors, but has a lower efficiency due to discontinuities in the depletion region along the waveguide.

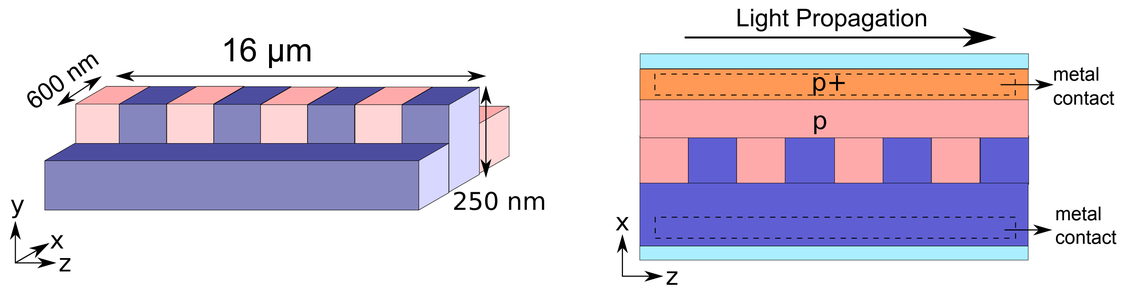

FIGURE 5: Interdigitated doping profile.

2D Monte Carlo Simulator

We develop 2D Monte Carlo simulator to evaluate the contribution of the ionization statistics to the jitter. The simulator calculates the avalanche current build up following a photon absorption. We get random photon injection positions from the cumulative distribution function obtained from time integral of the incident light. Due to different charge carrier transport dynamics, we set an electric field threshold to define the depletion layer, p-type and n-type quasi-neutral layers. If the injection happens into one of these neutral layers, then we solve the drift and diffusion equations using local field and diffusion coefficients for the minority electrons and holes in the p-type and n-type quasi-neutral layers, respectively. Following their diffusion into the depletion layer, we solve the location and time at which they cause an impact ionization.

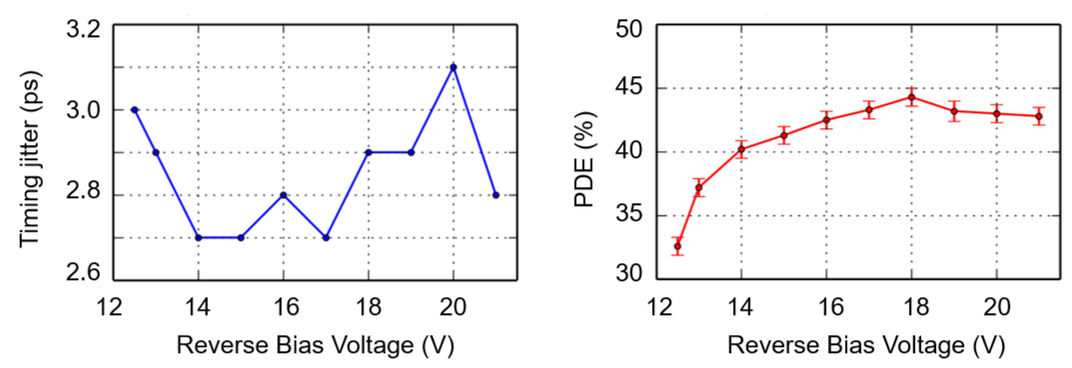

FIGURE 6: Simulated jitter and PDE for a device with straight doping profile and 600 nm width.

Since our design accomodates a narrow junction and the field exhibits a strong gradient, we resort to the non-local approach in ionization coefficients. To extract the random location where the ionization occurs, first we assign each charge carrier a random number that is uniformly distributed between 0 and 1 [4]. Then we compare that number with the cumulative ionization probability for that charge carrier at each step. If the cumulative probability is lower than that random number no ionization occurs, otherwise an impact-ionization takes place and a new electron-hole pair is created in the current position. The same steps are taken for newly generated charge carriers until the resulting current exceeds the detection threshold. Multiple avalanches are simulated and time to detection delays are sorted into time bins. Jitter information is taken to be the FWHM of the resulting histogram plot and PDE is taken to be the ratio of the number of the detection events to the number of photon injections (Fig. 6). The simulator uses the local ionization and diffusion coefficients and the mobilities. We obtained these parameters from the TCAD model (Silvaco) of the device, which uses the carrier photo-generation rate (Fig. 4b) obtained from 3D FTDT (Lumerical) simulations. We also calculate the spatial map of the avalanche trigger probability with these parameters (Fig. 4a).

Forthcoming Research

We will fabricate the SPADs with different waveguide widths of 450 nm, 600 nm, 750 nm and 900 nm. We will then characterize their photon detection efficiency, dark count rate, and timing jitter. The designs will be optimised for visible wavelenghts.

References

[1] A. Sipahigil et al., *An integrated diamond nanophotonics platform for quantum-optical networks*, Science **354**, 6314 (2016)
[2] D.J. Moss et al., *New CMOS-compatible platforms based on silicon nitride and Hydex for nonlinear optics*, Nat. Phot. **7**, 8 (2013)
[3] L. Tsung-Yang et al., *Silicon modulators and germanium photodetectors on SOI: monolithic integration, compatibility, and performance optimization*, IEEE JSTQE **16.1**, 307-31 (2010)
[4] A. Ingargiola et al., *Avalanche buildup and propagation effects on photon-timing jitter in Si-SPAD with non-uniform electric field*, Proc. SPIE **7320**, (2009)